Probabilistic Bridge Weigh-in-Motion

Eugene J. OBrien[a,e] Longwei Zhang[b,e], Hua Zhao[c], Donya Hajializadeh[d, *]

[a] *School of Civil Engineering, University College Dublin, Belfield, Dublin 4, Ireland*

[b] *Hunan Provincial Communications Planning, Survey & Design Institute Co., LTD, Changsha, Hunan, China*

[c] *Key Laboratory for Wind and Bridge Engineering of Hunan Province, Hunan University, Changsha, Hunan, China*

[d] *Department of Engineering & the Built Environment, Faculty of Science & Technology, Anglia Ruskin University, Essex, United Kingdom*

[e] *These authors contributed equally to this work and should be considered joint first authors*

* corresponding author: email, Donya.hajializadeh@anglia.ac.uk

Abstract

Conventional bridge weigh-in-motion (BWIM) uses a bridge influence line to find the axle weights of passing vehicles that minimize the sum of squares of differences between theoretical and measured responses. An alternative approach, probabilistic bridge weigh-in-motion (pBWIM), is proposed here. The pBWIM approach uses a probabilistic influence line and seeks to find the most probable axle weights, given the measurements. The inferred axle weights are those with the greatest probability amongst all possible combinations of values. The measurement sensors used in pBWIM are similar to BWIM, containing free-of-axle detector (FAD) sensors to calculate axle spacings and vehicle speed and weighing sensors to record deformations of the bridge. The pBWIM concept is tested here using a numerical model and a bridge in Slovenia. In a simulation, two hundred randomly generated 2-axle trucks pass over a 6 m long simply supported beam. The bending moment at mid-span is used to find the axle weights. In the field tests, seventy-seven pre-weighed trucks traveled over an integral slab bridge and the strain response in the soffit at mid-span was recorded. Results show that pBWIM has good potential to improve the accuracy of BWIM.

1. Introduction

As the main imposed loads on a bridge, the weights of vehicles play an important role in determining its safety (Yu et al. 2016). With increasing vehicle loading and a generally ageing bridge stock in the developed world, many existing bridges have suffered substantial deterioration which will shorten their service lives (Lydon et al. 2016). Road authorities sometimes use weigh-in-motion (WIM) systems to get information about the traffic acting on bridges and to inform them about the requirements for enforcement of the maximum weight limits (Blab and Jacob 2000). With 56% of bridges assessed every three years in Canada (Canadian Infrastructure 2016), utilizing accurate weighing systems could result in significant savings.

According to Zhang et. al 2007, WIM was first introduced to Canada in Alberta in 1982 and its usage has been increasing steadily. There are two categories of WIM system: pavement-based WIM and bridge WIM (BWIM). Pavement-based WIM systems utilize sensors embedded in the pavement to measure the instantaneous forces while the tire passes over the sensors (Jacob 1999, Jacob et al 2002). BWIM systems, first developed by Moses (1979), use an existing bridge as a scale to find the weights of vehicles passing overhead. In Moses' approach, BWIM is made up of two parts. One part consists of axle detectors monitoring axle numbers, spacings and vehicle speed. The other part consists of weighing sensors, usually strain transducers, recording the deformation of the bridge while vehicles cross over.

Both types of WIM system can take measurements directly and calculate axle weights while vehicles are moving at full highway speed (Richardson et al. 2014). Due to the very short recording time and vehicle-pavement dynamics, the accuracy of pavement-based WIM systems is limited by the width of the sensors and the roughness of the road profile (González 2010). In contrast, BWIM systems use the continuous response of the bridge for the time the vehicle takes to pass overhead. The response measurement period is much greater than the recording time for pavement-based WIM systems. This makes BWIM much less sensitive to vehicle dynamics and gives it the potential

for greater accuracy, especially on rough roads. BWIM systems also have other advantages over pavement-based WIM systems in terms of durability and portability (OBrien et al. 1999) but there will always be the limitation that a bridge is required at the site of interest.

Modern commercial BWIM systems are based on Moses' algorithm and variations of it (OBrien et al. 2008). To find axle weights, an error function E (Eq. 1), is defined as the sum of squares of differences between the measured and theoretical responses caused by passing vehicles (Moses 1979):

$$E = \sum_{i=1}^{K} [R_i^M - R_i^T]^2 \quad (1)$$

where i is the scan number; K is the total number of scans; R_i^M and R_i^T are the measured and theoretical response respectively at scan i. In the original Moses' algorithm, the theoretical response is taken as the sum of products of axle weights and the corresponding theoretical influence line ordinates. The theoretical influence line is now known to provide a poor representation of the real behavior of a bridge, so a modified influence line based on measurements is applied to improve accuracy. Žnidarič and Baumgartner (1998) adjusted the support conditions and smoothed the peaks to get an influence line of better consistency with the real situation. McNulty and OBrien (2003) developed a 'point-by-point' graphical method of manually deriving the influence line. OBrien et al. (2006) improved on this by proposing a 'matrix' method of calculating the 'measured' influence line ordinates that best fit the response to a calibration truck of known axle weights. In effect, the error function of Eq. 1 is minimized to determine the unknown influence ordinates as opposed to the axle weights.

In the United States and Canada there have been several studies in the improvement of the accuracy of BWIM methods since Moses' early work. For example Bakht et al. (2006) tested the accuracy of the reaction force theory developed by Yamada & Ojio (2003) using an instrumented bridge in Manitoba. Their study shows a high sensitivity of strains to transverse position of the

vehicle on the bridge and hence inaccurate axle weights for trucks in certain transverse positions. Helmi et al. (2014) conducted a comparative study of three BWIM methods. In two of these the truck load is represented by an equivalent uniformly distributed load and in the third GVW is estimated using strain signal area as proposed by Yamada & Ojio (2003). The study found inconsistency in accuracy in the first method, reduced accuracy with vehicle length in the second and less than 5% error in GVW in the third. Faraz et al. (2017) reported similar results for these techniques when identifying sources of error in the fatigue evaluation of South Perimeter Bridge. The BWIM method developed by (Wall et al. 2009) builds on the (Yamada & Ojio 2003) theory and (Cardini & DeWolf 2007) study to determine gross vehicle weight, speed, axle spacing, and axle weights. The results has shown, that 95% confidence interval of GVW varies from 6.31% to +-15.20% for two lanes of a simply supported steel girder bridge with a concrete deck slab.

Despite these efforts to improve the standard practices and the accuracy, there are challenges associated with current BWIM technologies. Previous research shows that gross vehicle weights (GVWs) have greater accuracy than individual axle weights in BWIM (Žnidarič et al 2008; Zhao et al. 2015). This is mainly due to the ill-conditioning of the BWIM equations, especially for closely spaced axles and/or long bridges. The method of Tikhonov regularization has been successfully applied to reduce some of the inaccuracies in axle weights (OBrien et al. 2009; Rowley et al. 2008). However, the procedure of getting the optimal regularization parameter is complex and subjective.

To further improve the accuracy of BWIM, moving force identification (MFI) theory was developed by Law et al. (1997). MFI can obtain the time-history of applied axle forces using an accurate vehicle-bridge interaction finite element (FE) model. Dowling et al. (2012) have addressed the problem of calibrating the system, similar to the issue of finding the measured influence line in conventional BWIM. Although experimental tests showed that MFI has the potential to improve

accuracy, it is computationally demanding and some have suggested that it is impractical (Deng and Cai 2010; Rowley et al. 2009).

This study proposes a novel probabilistic BWIM algorithm (pBWIM), which addresses the uncertainty in the influence line by representing it probabilistically. In pBWIM systems, it is assumed that each influence line ordinate can be represented by a normal distribution. The probability of a given measurement is calculated for all possible combinations of axle weights. The combination of axle weights with the highest probability of occurrence, given the measurements recorded, is taken as the calculated result. Both numerical modeling and field testing are used here to test the pBWIM algorithm. The axle weights are also obtained by conventional BWIM and the corresponding accuracies are compared.

2. Theory and Numerical Modeling

2.1 *pBWIM algorithm*

An influence line (IL) is an inherent property of a bridge that describes its response to unit load. It depends on bridge length, elastic modulus, boundary conditions, etc. In conventional BWIM, the so called 'measured IL' is directly obtained from the calibration tests with vehicles of known weights by finding the influence ordinates that minimize the differences between theoretical and measured responses (OBrien et al. 2006). There is a measured IL corresponding to every run with a vehicle of known weight. The average of all such measured ILs can then be used to calculate axle weights.

In this paper, it is assumed that each measured IL ordinate (I_i) follows a normal distribution ($[\mu_i^I, \sigma_i^I]$), where μ_i^I and σ_i^I are the mean and standard deviation of the measured IL ordinate respectively for scan i, obtained by field tests. When vehicles pass over the bridge, the measurements (strains or displacements) are recorded by the monitoring system. The axle number and axle spacings can be found by using a free-of-axle detector (FAD) or nothing-on-the-road (NOR) system (Kalin et al. 2006; Zhao et al. 2013). Due to the uncertainty of each axle weight in

a vehicle, there are many hundreds of possible combinations of the axle weights ($\mathbf{W}^k$), where $\mathbf{W}$ is the axle weight vector and $\mathbf{W}^k$ is the k^{th} possible combination of $\mathbf{W}$. The theoretical response (R_i) for the i^{th} scan is the sum, for each axle, of the products of axle weights and the corresponding influence line ordinates:

$$R_i = W_1 I_i + W_2 I_{i-D_2} + ... + W_n I_{i-D_n} + E^M \tag{2}$$

where n is the number of axles, D_j is the number of scans corresponding to the distance between the j^{th} axle and the first axle, and E^M is zero mean random measurement noise. As the response is a linear combination of normal random variables, it too is normally distributed. Hence, for each combination of axle weights ($\mathbf{W}^k$), the response (R_i) follows a specific normal distribution ($[\mu_i^k, \sigma_i^k]$), where μ_i^k and σ_i^k can be calculated by Eq. 3:

$$\begin{aligned} \mu_i^k &= W_1^k \mu_i^I + W_2^k \mu_{i-D_2}^I + ... + W_n^k \mu_{i-D_n}^I \\ \sigma_i^k &= \sqrt{(W_1^k \sigma_i^I)^2 + (W_2^k \sigma_{i-D_2}^I)^2 + ... + (W_n^k \sigma_{i-D_n}^I)^2 + (\sigma^M)^2} \end{aligned} \tag{3}$$

where σ^M is the standard deviation of measurement noise, which is a constant. Based on a given combination of axle weights ($\mathbf{W}^k$) and the corresponding normal distribution ($[\mu_i^k, \sigma_i^k]$), the probability of the response ($P^k(R_i)$) at scan i can be calculated by Eq. 4:

$$\begin{aligned} f^k(R_i) &= \frac{1}{\sigma_i^k \sqrt{2\pi}} e^{\frac{-(R_i - \mu_i^k)^2}{2(\sigma_i^k)^2}} \\ P^k(R_i) &= \int_{R_i - \Delta_R/2}^{R_i + \Delta_R/2} f^k(R) dR \end{aligned} \tag{4}$$

where $f^k(R)$ and Δ_R are probability density and the interval of response respectively. Due to the small value of Δ_R, $f^k(R)$ can be taken as constant ($f^k(R_i)$) in the range [$R_i - \Delta_R/2$, $R_i + \Delta_R/2$]. The probability, $P^k(R_i)$ can then be rewritten as Eq. 5:

$$P^k(R_i) = \Delta_R \bullet f^k(R_i) \tag{5}$$

If the influence ordinates are assumed to be independent, the probability of the response having their recorded values ($P(\mathbf{R})$) is the product of probabilities for all the measurement points:

$$P(\mathbf{R}) = \prod_{i=1}^{K} P(R_i) = (\Delta_M)^K \bullet \prod_{i=1}^{K} f(R_i) \tag{6}$$

where K is the total number of scans in the measured response.

For a specific measured response, the axle number and spacing can be obtained by a FAD system. There will be many possible combinations of axle weights. For a combination (k), there is a corresponding probability ($P^k(\mathbf{R})$) of the measurement. The magnitude of the probability depends on the mean (μ_i^k) and standard deviation (σ_i^k) of the theoretical response. It is known from Eq. 3 that μ_i^k and σ_i^k are a function of the axle weights, the mean of the influence line (μ_i^I) and its standard deviation (σ_i^I). Among them, μ_i^I and σ_i^I are constant, and axle weights are the independent variables. Thus, the combination of axle weights plays a significant role in determining $P^k(\mathbf{R})$. In pBWIM, the probability of this response is found and the combination of axle weights with the greatest probability is the inferred result.

2.2 *Example*

2.2.1 *Numerical model description*

To verify the theory of pBWIM, a simple static vehicle-bridge model was developed. The model is shown in Figure 1 and is for a 2-axle truck passing over a simply supported beam. The bridge length is 6 m. The bending moment at mid-span is taken as the response (R_i), which can be calculated from Eq. 7:

$$R_i = W_1 I_i + W_2 I_{i-D_2} + E^M \tag{7}$$

where I_i is the influence line with an allowance for random error, and E^M is measurement noise. It is noted that the simulated measurement excludes dynamic vehicle-bridge interaction. The

response is the sum of the products of the axle weights and the corresponding IL ordinates for each axle and a random measurement noise.

For this theoretical example, the mean value (μ_i^I) equals the theoretical influence line. The standard deviation (σ_i^I) has been taken as a simple proportion of the maximum, i.e., $\lambda \times \max\{\mu_i^I\}$, where λ is the scale factor, typically taken as 0.1, i.e. 10% (González et al. 2008). Figure 2 shows the comparison between the theoretical IL and the IL with random error.

The measurement noise (E^M) is simulated as additive white Gaussian noise (AWGN), which is caused by a measurement source, using Eq. 8 (Yabe and Miyamoto 2012, Keenahan et al. 2014).

$$E^M = E_{noise} \times U$$
$$SNR = 10\log_{10}\frac{\mathrm{var}(R^*)}{E_{noise}^2} \tag{8}$$

where U is a standard normal distribution vector with zero mean and unit standard deviation. E_{noise} is the energy in the noise, which is determined by the ratio of the power (SNR) in the noise. Measurement noise at an SNR level of 30 is added in this paper. $\mathrm{var}(R^*)$ is the variance of the response (R^*).

In this paper, 200 random 2-axle vehicles are generated and passed over the simply supported bridge. The axle weights and spacings respectively are generated from the normal distributions, specified in Eq. 9.

$$GVW \sim N(130,\ 13),\quad GVW > 0\,\mathrm{kN}$$
$$W_1/GVW \sim N(0.25,\ 0.03),\quad 0 < W_1 < GVW \tag{9}$$
$$S \sim N(5, 0.5),\quad S > 2\,\mathrm{m}$$

where GVW is the gross vehicle weight, W_1 is the first axle weight, and S is the axle spacing. Using the vehicle information, the simulated and theoretical response to each vehicle can be calculated where the simulated response includes noise (influence line + measurement noise) and the theoretical response does not. Figure 3 shows the simulated and theoretical responses at mid-span for a typical 2-axle truck. The simulated response varies around the corresponding theoretical one.

2.2.2 *Calculation*

In pBWIM, the probability of the measurement signal is used to get the axle weights. For the comparison, axle weights are also obtained from Moses' algorithm (conventional BWIM) using the theoretical IL. Figure 4 is a flowchart showing a series of simulations, including the pBWIM procedure which incorporates conventional Moses' BWIM.

Firstly, the simulated bending moment at mid-span is calculated based on the two axle weights, spacing, the random IL and measurement noise for each vehicle using Eq. 7. Then, axle weights are calculated using pBWIM and Moses' algorithms. In Moses' algorithm, axle weights are obtained by minimizing the error function of Eq. 1 where the 'measurement' is calculated using Eq. 7. In pBWIM, the calculated axle weights $< \hat{W}_1, \hat{W}_2 >$ are those with the highest probability of occurrence among all possible combinations of axle weights. To improve the efficiency of calculation, each axle weight is restricted to the range of [0.8, 1.2] times Moses' values, in increments of 0.1 kN. This is reasonable as the results of Moses' algorithm are close to the true values (Richardson et al. 2014). The probabilities of measurement for all the combinations can be obtained by Eq. 4 to Eq. 6. For this example, contours of probability are plotted in Figure 5 for a typical vehicle for which the true weights are $<W_1, W_2>$ = <51, 80> kN. It is can be seen that the most probable result is at <51.2, 79.8> kN, which is very close to the true value.

A1: kN

2.2.3 *Results and Analysis*

The procedures above are repeated for 200 simulated measurements. The mean errors and standard deviations are obtained for the weights of each axle, gross vehicle weight (GVW) and single axle weight, taken collectively for the two axles. The results from these simulations are listed in Table 1.

As can be seen, although the mean error and standard deviation of each entity are similar for the two algorithms, the mean error and standard deviation are slightly less when applying the

pBWIM algorithm. For example, the mean error in the prediction of single axle weight decreases from 0.23% to 0.17%, and the standard deviation decreases from 2.38% to 2.21%. The biggest drop happens in the first axle. The mean error and standard deviation are reduced from 0.22% and 2.53% respectively to 0.15% and 2.27% when using pBWIM algorithm. Hence, for the numerical model considering the random error in the influence line and measurement noise, both algorithms are excellent with pBWIM improving the accuracy a little relative to Moses' algorithm.

3. Field Test

In the simulations, most of the results were very good which made it hard to clearly identify the differences between the two algorithms. For this reason, a field test was sought, for which the results were poor. The objective was to determine if poor results from Moses' algorithm could be improved with pBWIM. The Sentvid Bridge in Slovenia was selected because it was located on a stretch of road where the surface profile was not good and Moses' algorithm was giving results well below the level of accuracy that is typical of BWIM (Corbally and Žnidarič 2013).

3.1 *Site Layout*

The Sentvid bridge is a frame/culvert type of structure as shown in Figure 6. The bridge consists of two independent structures, each of which is 6 m long and 6.25 m wide, carrying two lanes of traffic.

The hardware components of the pBWIM system are the same as for conventional BWIM. Each bridge structure is instrumented with 16 strain transducers, consisting of 4 FAD transducers and 12 weighing transducers. Figure 8 shows the layout of the transducers for one bridge structure. The FAD transducers (7-8 and 15-16) are mounted 4 m apart in the longitudinal direction, two underneath each traffic lane. They are used for axle detection and speed calculation. The weighing transducers (1-6 and 9-14) are installed at mid-span with equal transverse spacings of 0.5 m.

During the field tests, the test vehicles traveled in Lane 1 (corresponding to the slow-lane shown in Figure 7). All the vehicles were pre-weighed at a static weigh station. There are 77 measurements recorded in total, as listed in Table 2.

3.2 *Selected sensor*

Comparing the accuracy of the calculated weights using individual sensors showed that the sensors, which were located underneath Lane 1, in which all the trucks traveled, provided the best accuracy. Figure 8 shows a comparison of the accuracy of the calculated GVWs where just one of the weighing sensors is used in the BWIM algorithm in each case. The X-axis shows the transverse spacings between the sensors used in the calculation and the Y-axis shows GVW accuracy, with 100% indicating an exact prediction. The horizontal dashed lines correspond to the goals set by Corbally and Žnidarič (2013) – see caption.

It can clearly be seen that the most consistent accuracy was obtained when the sensors underneath the lane were used for weighing (notably, sensor 5 located at 3 m gave the best accuracy). Some sensors give far more variability in the accuracy of the results (e.g. the predictions from sensor 14 are very inconsistent). This results from the fact that the sensors further away from Lane 1 have smaller magnitude and are therefore more sensitive to noise/disturbances in the signals. Based on these results it was proposed that a single sensor BWIM algorithm should be tested here using only sensor 5 for the weighing of vehicles in Lane 1. It should be noted that accuracy might be improved by utilizing more sensors.

3.3 *Measured ILs*

The measured IL derived by the matrix method was adopted (OBrien et al. 2006). In this case, the axle weights of the pre-weighed trucks and measured responses are known, so the IL ordinates can be found by minimizing E in Eq. 1.

As the Sentvid Bridge is an integral box culvert, vehicular load on the approach produces a load effect on the bridge at mid-span. When calculating the measured influence line, an approach length of 2 m is considered. Hence the total length of the influence line consists of bridge length and two approaches, totaling 10 m (2 + 6 + 2 =10). Figure 9 shows the measured influence lines for all test trucks.

It can be seen that all influence lines have a similar shape, and the peak values fall into the approximate range [0.04, 0.07]. Figure 10 presents the histogram and a normal distribution fit to the peak values. The data of Figure 10 matches well to a normal probability density function as can be seen from the straight line fit of Figure 10b.

A Kolmogorov-Smirnov test (Massey 1951) is used to check every point in the influence lines for compliance with a specific normal distribution. Results show that 90% of all points in the influence lines follow normal distributions at the 5% significance level. In this paper, it is assumed that all influence ordinates follow the normal distribution. The calculated means and standard deviations for each point on the influence line are shown in Figure 11.

3.4 *Finding axle weights*

In pBWIM, the procedure for determining axle weights from the measurements is similar to that used for the numerical model. The process is illustrated in Figure 12. For each measurement, the axle weights are first obtained with Moses' algorithm. The Moses' results are then used to determine each approximate axle weight and hence to generate the range used to generate the combinations to be tested in the pBWIM algorithm. Each axle weight is constrained to the range [0.8, 1.2] times the corresponding Moses' values, and the increment adopted is 0.1 kN. As the influence line ordinates are normally distributed, the theoretical response, being a linear combination, should follow a specific normal distribution for each combination of axle weights. For each combination of axle weight, the mean (μ_i^k) and standard deviation (σ_i^k) of the response at scan *i* can be calculated by Eq. 3. The standard deviation of measurement noise (σ^M) is taken here as zero. Using μ_i^k and σ_i^k, the probability of the response ($P^k(\mathbf{R})$) can be calculated using Eqs. 4 to 6. Finally, the combination of axle weight ($\mathbf{W}^P$) with the highest probability is found.

4 Field Testing

4.1 *Results with High-accuracy Influence Line*

In an initial test, referred to as Case 1, a high-accuracy influence line (IL) is utilized. For this case, the mean of all measured influence lines is used for both Moses' BWIM algorithm and to find the mean and standard deviation for the pBWIM algorithm. It is acknowledged that such a good IL would not normally be available in real field conditions.

For each measurement entity, the mean and standard deviation of the relative mean errors are calculated and are listed in Table 3.

For this bridge, the results from Moses' BWIM algorithm can be seen to be excellent. The mean absolute error for each entity is greater when using the probabilistic algorithm, though the corresponding standard deviation is less. For instance, the mean absolute error in the prediction of the single axle weight increases from 0.022% to 3.58%; the standard deviation decreases from 13.31% to 12.45%.

To get an insight into the distributions of accuracy for the two algorithms, the details of GVW errors versus vehicle number are plotted in Figure 13. This shows that most GVW errors from pBWIM are less than (often 'more negative than') the errors from BWIM. When the GVW errors are above zero, the predicted GVW's from pBWIM are consistently less. Overall, the errors in both algorithms are small and similar, with BWIM consistently outperforming pBWIM. The likely reason is that the mean IL from all test trucks was used. As such, the uncertainty in the IL was low. The potential for pBWIM to deal with IL uncertainty was therefore not realized in this case.

4.2 *Results with Inaccurate Influence Lines*

Based on the results from the first field test case, pBWIM does not have an obvious advantage over conventional BWIM. However, it will be shown here that pBWIM can deal better with inaccurate IL's. To be more realistic, the IL is obtained here from a small number of calibration test runs, and this low-accuracy IL is used to calculate the weights of trucks passing over the bridge. In addition

to the case already considered, two further cases are considered here for the pBWIM and BWIM algorithms.

Case 2: The IL is taken here as the mean of the 10 measured ILs with the smallest peaks. For pBWIM, two variations are considered. For Case 2a, the means and standard deviations of the 10 ILs with the smallest peaks are used to calculate the probabilities. For Case 2b, the same means are used but the standard deviations are based on *all* measured ILs.

Case 3: Here the IL is taken from the 10 measured ILs with the greatest peaks. Similar to above, Case 3a calculates the standard deviations from the 10 ILs with greatest peaks while Case 3b calculates them from all measured IL's.

The results are listed in Table 4.

For Cases 2a and 2b, it can be seen that both the mean errors and the standard deviations from pBWIM are less than the mean errors and standard deviations from BWIM. This is true for all entities: GVW, groups of axles and single axles. It should be noted that the mean IL for pBWIM is the same IL as used for BWIM. Clearly allowing for the variability in IL reduces the sensitivity of pBWIM to influence line accuracy. Further, the standard deviation for IL used in pBWIM is important as can be seen by the differences in accuracies between Cases 2a and 2b (and similar for Cases 3a and 3b).

For Case 3a, the mean absolute error from pBWIM is greater than the mean from BWIM, but the standard deviation from pBWIM is less; For Case 3b, the mean absolute error and standard deviation from pBWIM are both less than for BWIM.

In pBWIM, with the same mean of the measured IL's, the more measured IL's that are used to get the standard deviations, the better pBWIM becomes, i.e., getting a good estimate of the true standard deviation of the IL is important for pBWIM accuracy. For example, in Case 2b where more accurate measures of the variability of the IL are used, the mean error with the pBWIM

algorithm falls to 5.5% for gross weights (from 8.15% with BWIM and 7.51% for Case 2a) and there are similar reductions for axle groups and single axle weights.

For all cases, both BWIM and pBWIM based on measured ILs can get the best accuracy. It can be inferred that BWIM and pBWIM will have similarly high accuracy if the data from the calibration are sufficient, i.e., if the IL is accurate. In comparison to BWIM, pBWIM is better able to cope with cases where the IL is not accurate.

5. Conclusion

This paper proposes a novel algorithm, probabilistic bridge weigh-in-motion (pBWIM), to calculate axle and vehicle weights. Unlike conventional BWIM that minimizes the squared difference between measured and predicted responses, pBWIM utilizes the probability of measurement to find the most probable axle weights. Numerical modeling and field testing are both used to evaluate the feasibility and accuracy of pBWIM. The simulations and measurements are also used to find axle weights using Moses' BWIM algorithm.

Results of the simulations show that both the mean absolute errors and standard deviations of calculated GVW, 1st and 2nd axle weights are less for pBWIM in comparison to the corresponding values using Moses' algorithm.

In the field tests, when using the average of all measured ILs to find axle weights, the mean absolute errors from pBWIM are slightly greater than the errors from BWIM, but the standard deviations from pBWIM are less. When using IL based on a subset of available results, as would be typical in a measurement campaign, pBWIM can get smaller mean absolute errors and standard deviations, i.e., pBWIM appears to be more tolerant of the fact that the IL is inaccurate.

This paper provides a proof of concept for what is, to the authors' knowledge, the first of its kind – namely, an entirely probabilistic bridge weigh-in-motion system.

Acknowledgements

This research was supported by the China Scholarship Council, National Natural Science Foundation of China (51178178), Science Foundation Ireland, the 7th Framework *BridgeMon* project and Hunan Provincial Natural Science Foundation of China (13JJ2019). These programs are gratefully acknowledged. Cestel, suppliers of the SiWIM BWIM system, is thanked for providing access to the *BridgeMon* data.

References

Bakht, B., Mufti, A.A., Tadros, G., Eden, R. and Mourant, G. 2006. Weighing-in-motion of truck axle weights by Japanese reaction force method. 3rd Int. In: *Conf. on Bridge Maintenance, Safety and Management*, Porto, Portugal, July. 16–19.

Blab, R., and Jacob, B. 2000. "Test of a multiple sensor and four portable WIM systems." *International Journal of Heavy Vehicle Systems*, 7(2-3), 111-135.

Canadian Infrastructure. 2016. Canadian infrastructure report card - informing the future, Available at:

http://www.canadainfrastructure.ca/downloads/Canadian_Infrastructure_Report_2016.pdf#page=28 [Accessed October 2, 2016].

Cardini, A.J. and DeWolf, J.T., 2007. *Development of a Long-Term Bridge Weigh-In-Motion System for a Steel Girder Bridge in the Interstate Highway System*. University of Connecticut.

Corbally, R. and Žnidarič, A. 2013. *Algorithm for Improved Accuracy Static Bridge-WIM System.* Deliverable D1.2, EU funded *BridgeMon* project (Bridge Monitoring), 2012 - 2014, GA no. 315629.

Deng, L., and Cai, C. 2010. "Identification of dynamic vehicular axle loads: Demonstration by a field study." *Journal of Vibration and Control*, 17(2), 183–195.

Dowling, J., OBrien, E. J, and González, A. 2012. "Adaption of cross entropy optimization to a dynamic bridge WIM calibration problem." *Engineering Structure*. 44, 13-22.

Faraz, S., Helmi, K., Algohi, B., Bakht, B. and Mufti, A., 2017. Sources of errors in fatigue assessment of steel bridges using BWIM. Journal of Civil Structural Health Monitoring, 7(3), pp.291–302.

González, A. 2010. *Development of a Bridge Weigh-In-Motion System*. Germany: LAP Lambert Academic Publishing AG & Co. KG.

González, A., Rowley, C., and OBrien, E. J. 2008. "A general solution to the identification of moving vehicle forces on a bridge". *International Journal for Numerical Methods in Engineering*, 75(3), 335–354.

Helmi, K., Bakht, B. and Mufti, A., 2014. Accurate measurements of gross vehicle weight through bridge weigh-in-motion: A case study. Journal of Civil Structural Health Monitoring, 4(3), 195–208.

Jacob, B. 1999. COST 323 Weigh in motion of road vehicles. Final Report, appendix 1 European WIM Specification, LCPC Publications, Paris.

Jacob, B., OBrien, E.J. and Jehaes, S. (Eds.) 2002, Weigh-in-Motion of Road Vehicles: Final Report of the COST 323 Action, LCPC Publications, Paris, 538.

Kalin, J., Žnidarič, A., and Lavrič, I. 2006. "Practical implementation of nothing-on-the-road bridge weigh-in-motion system." *Proc., 9th Int. Symp. on Heavy Vehicle Weights and Dimensions,* ARRB Group, Vermont South, VIC, Australia.

Keenahan, J., OBrien, E. J., McGetrick, P. J., & Gonzalez, A. 2013. "The use of a dynamic truck-trailer drive-by system to monitor bridge damping." *Structural Health Monitoring*, 13(2), 143–157.

Law, S., Chan, T. H., and Zeng, Q. 1997. "Moving force identification: a time domain method." *Journal of Sound and vibration*, 201(1), 1-22.

Lydon, M., Taylor, S., Robinson, D., Mufti, A., and Brien, E. 2016. "Recent developments in bridge weigh in motion (B-WIM)." *Journal of Civil Structural Health Monitoring*, 6(1), 69-81.

Massey, F. J. 1951 “The Kolmogorov-Smirnov Test for Goodness of Fit.” *Journal of the American Statistical Association*, 46(253), 68–78.

McNulty, P., and OBrien, E. J. 2003. “Testing of bridge weigh-in-motion system in sub-arctic climate.” *Journal of Testing and Evaluation*, 11(6), 1-10.

Moses, F. 1979. “Weigh-in-motion system using instrumented bridges.” *Transportation Engineering Journal*, 105(3), 233-249.

OBrien, E. J., Quilligan, M., and Karoumi, R. 2006. “Calculating an influence line from direct measurements.” *Bridge Engineering, Proceedings of the Institution of Civil Engineers*, 159(BE1), 31-34.

OBrien, E. J., Rowley, C. W., González, A., and Green, M. F. 2009. “A regularised solution to the bridge weigh-in-motion equations.” *International Journal of Heavy Vehicle Systems*, 16(3), 310-327.

OBrien, E. J., Znidaric, A., and Dempsey, A. T. 1999. “Comparison of two independently developed bridge weigh-in-motion systems.” *International Journal of Heavy Vehicle Systems*, 6(1-4), 147-161.

OBrien, E. J, Znidaric, A., and Ojio, T. 2008. “Bridge weigh-in-motion – Latest developments and applications worldwide.” *Proceedings of the International Conference on Heavy Vehicles HVTT10*, Eds. B. Jacob, E. OBrien. A. O’Connor, M. Bouteldja, Wiley, 2008, 39-56.

Richardson, J., Jones, S., Brown, A., OBrien, E., and Hajializadeh, D. 2014. “On the use of bridge weigh-in-motion for overweight truck enforcement.” *International Journal of Heavy Vehicle Systems*, 21(2), 83-104.

Rowley, C., Gonzalez, A., OBrien, E., and Znidaric, A. 2008. “Comparison of conventional and regularized bridge weigh-in-motion algorithms.” *Proc., Proceedings of the International Conference on Heavy Vehicles*, Eds. B. Jacob, E. OBrien, A. O'Connor, M. Bouteldja, Wiley, 2008, 271-282.

Rowley, C., OBrien, E. J., González, A., and Žnidarič, A. 2009. "Experimental testing of a moving force identification bridge weigh-in-motion algorithm." *Experimental Mechanics*, 49(5), 743-746.

Wall, C.J., Christenson, R.E., Mcdonnell, A.-M.H. and Jamalipour, A., 2009. A Non-Intrusive Bridge Weigh-in-Motion System for a Single Span Steel Girder Bridge Using Only Strain Measurements, Rep. SPR-2251, 7.

Yabe A and Miyamoto A. 2012. "Bridge condition assessment for short and medium span bridges by vibration responses of city bus." *In: Proceedings of the sixth international conference for bridge maintenance and safety*, London, UK: CRC Press, Taylor and Francis Group, 195–202.

Yamada, K. and Ojio, T., 2003. "Bridge weigh-in-motion system using reaction force method". In: Proc. of the Int. Workshop on Structural Health Monitoring of Bridges/Colloquium on Bridge Vibration. 269–276.

Yu, Y., Cai, C., and Deng, L. 2016. "State-of-the-art review on bridge weigh-in-motion technology." *Advances in Structural Engineering*, 19 (9), 1514-1530.

Zhang, L., Haas, C. and Tighe, S.L., 2007. "Evaluating weigh-in-motion sensing technology for traffic data collection". In *Annual Conference of the Transportation Association of Canada* (pp. 1-17).

Zhao, H., Uddin, N., OBrien, E. J., Shao, X., and Zhu, P. 2013. "Identification of vehicular axle weights with a Bridge Weigh-in-Motion system considering transverse distribution of wheel loads." *Journal of Bridge Engineering*, 19(3): doi: 10.1080/15732479.2014.904383.

Zhao, H., Uddin, N., Shao, X., Zhu, P., and Tan, C. 2015. "Field-calibrated influence lines for improved axle weight identification with a bridge weigh-in-motion system." *Structure and Infrastructure Engineering,* 22(6), 721-743.

Žnidarič, A., and Baumgartner, W. 1998. "Bridge weigh-in-motion systems – an overview."*: Pre-proceedings of the 2nd European Conference on Weigh-in-Motion of Road Vehicles,* Eds. E. J. OBrien & B. Jacob, Lisbon, Sep., European Commission, Luxembourg 139-151.

Žnidarič, A., Lavrič, I., and Kalin, J. 2008. "Measurements of bridge dynamics with a bridge weigh-

in-motion system." *Proc., 5th Int. Conf. on Weigh-in-Motion*, B. Jacob, E. J. OBrien, A. O'Connor, and M. Bouteldja, eds., ISTE Publishers, Paris, 388–397.

Tables

Table 1: Error percentages of mean and standard deviation for two algorithms

Entity	Moses' Algorithm		pBWIM Algorithm	
	Mean (%)	Standard deviation (%)	Mean (%)	Standard deviation (%)
1st axle	0.22	2.53	0.15	2.27
2nd axle	0.24	2.22	0.18	2.16
GVW	0.24	2.21	0.18	2.17
Single axle	0.23	2.38	0.17	2.21

Table 2 Distribution of test vehicles by axle number

Type	2-axle	3-axle	4-axle	5-axle	6-axle
No. trucks	8	8	7	52	2

Table 3: Mean errors and standard deviation for each algorithm in Case 1

Entity	Probabilistic BWIM Algorithm		Moses' BWIM Algorithm	
	Mean (%)	Standard deviation (%)	Mean (%)	Standard deviation (%)
GVW	-2.39	5.91	-0.065	6.21
Group of axles	-1.87	8.22	-0.49	8.61
Single axle	-3.58	12.45	-0.022	13.31

Table 4: Relative errors for each algorithm for Cases 2 and 3

Algorithm		GVW		Group of axles		Single axle	
		Mean (%)	Standard deviation (%)	Mean (%)	Standard deviation (%)	Mean (%)	Standard deviation (%)
Case 2	BWIM	8.15	6.72	7.94	9.83	6.85	17.42
Case 2a	pBWIM	7.51	6.65	7.05	9.63	6.63	17.33
Case 2b	pBWIM	5.50	6.38	6.40	9.69	3.05	16.95
Case 3	BWIM	-6.87	5.82	-7.13	8.07	-7.07	12.33
Case 3a	pBWIM	-7.56	5.78	-7.19	7.97	-8.57	12.26
Case 3b	pBWIM	-6.51	5.70	-6.42	7.91	-7.06	12.09

Figures

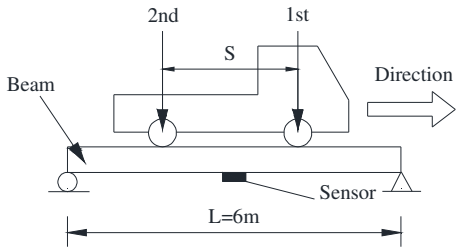

Figure 1: 2-axle truck passing over a simply supported beam

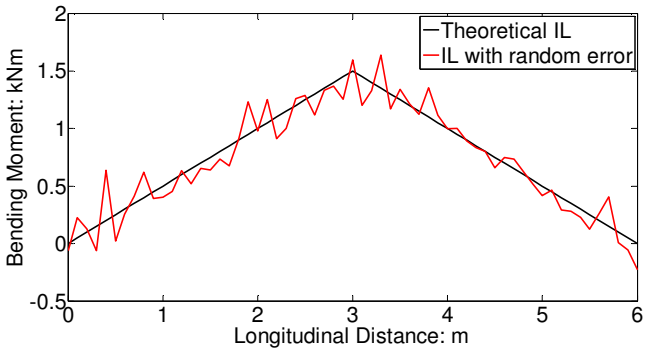

Figure 2: Noisy and theoretical influence lines

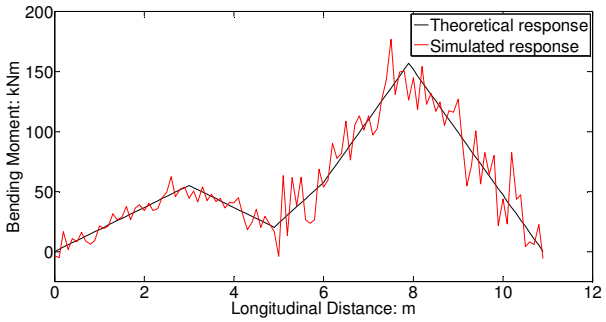

Figure 3: Simulated and theoretical responses at mid-span

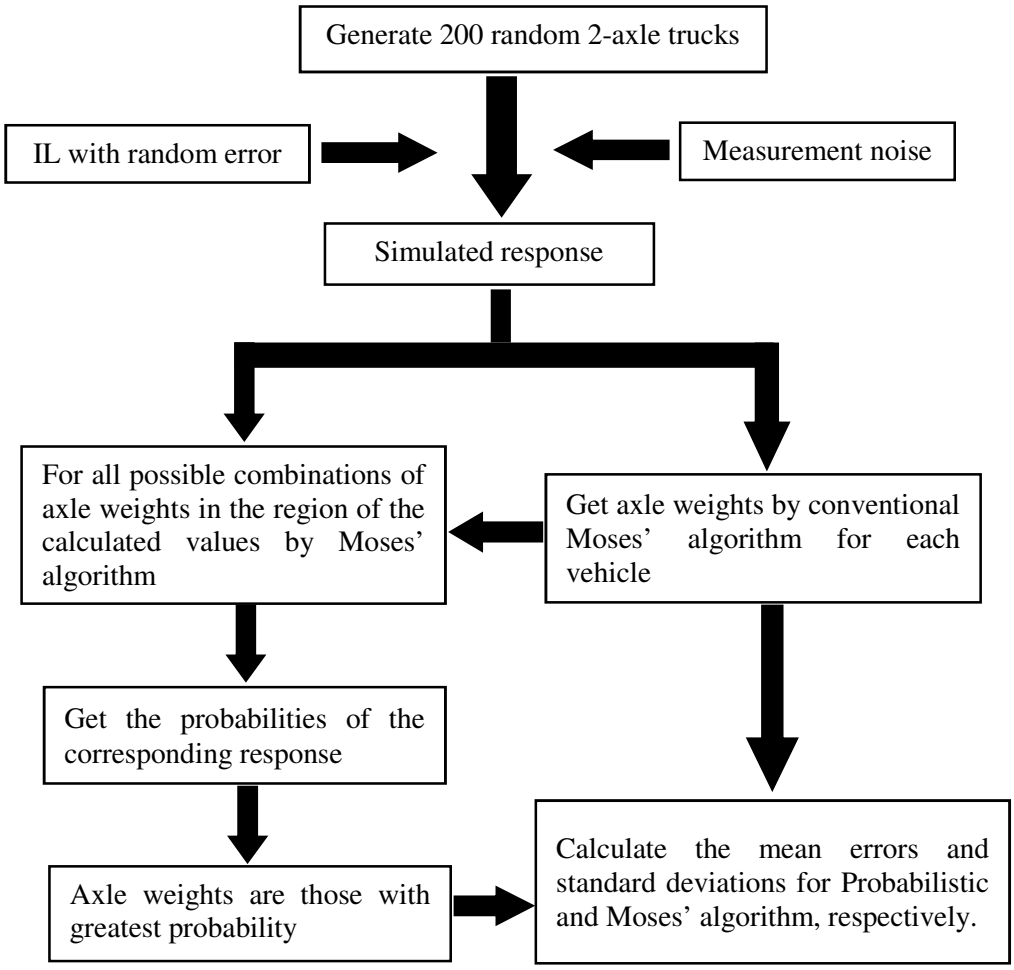

Figure 4: Flow chart for calculating axle weights using probabilistic algorithm and comparing them to Moses' algorithm

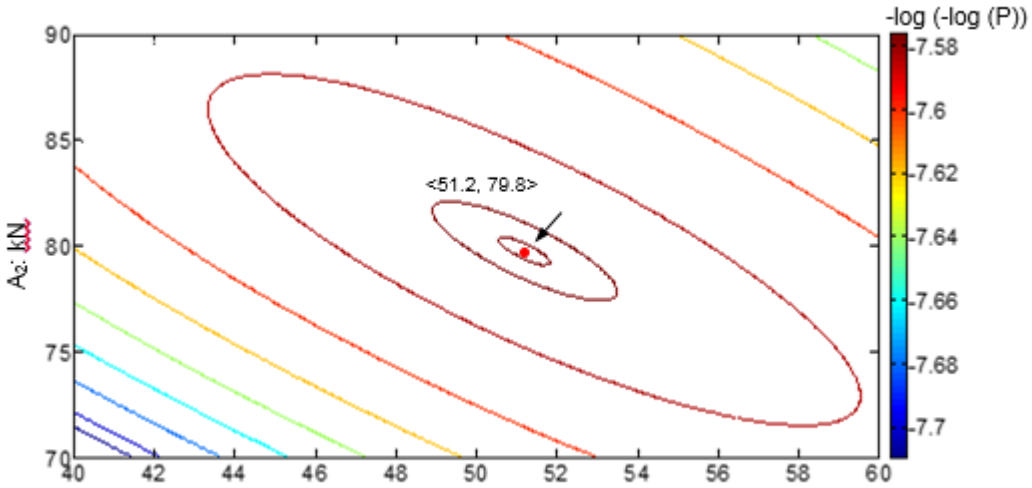

Figure 5: Contours of probability for all combinations of axle weights considered

Figure 6: Sentvid Bridge

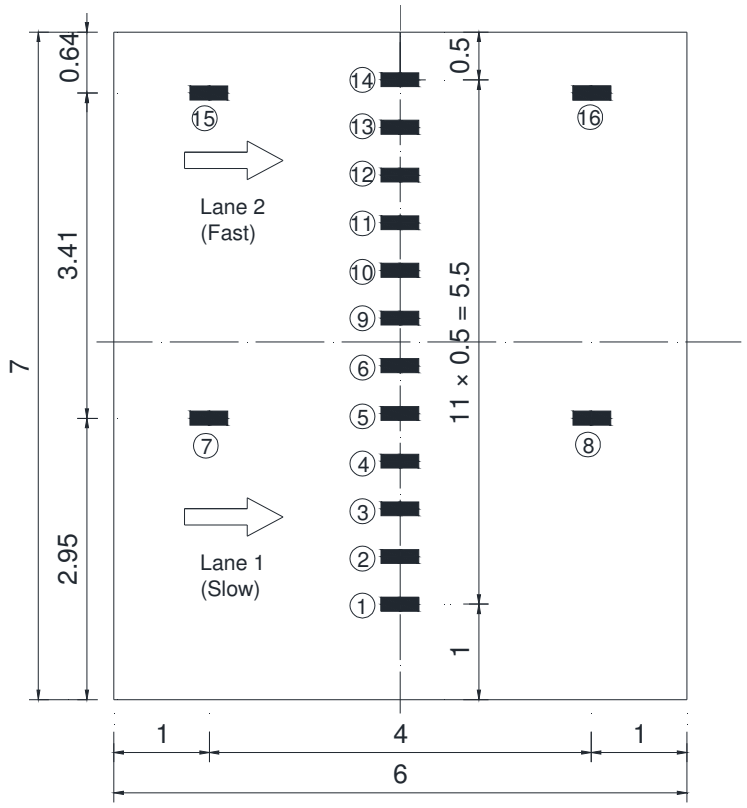

Figure 7: Plan layout of transducers (7, 8, 15, 16 for FAD, all others for weighing) unit: m

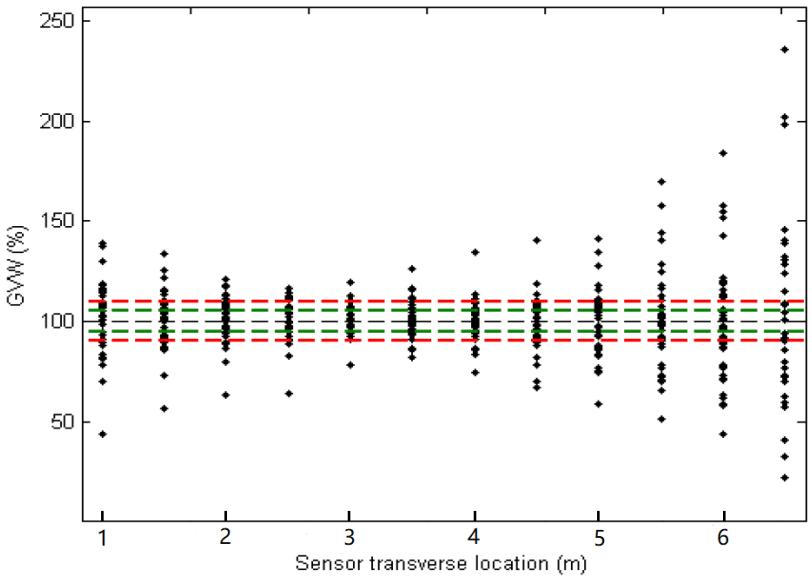

Figure 8: GVW accuracy for each sensor (green ±5% error, red ±10% error) (Corbally and Žnidarič 2013)

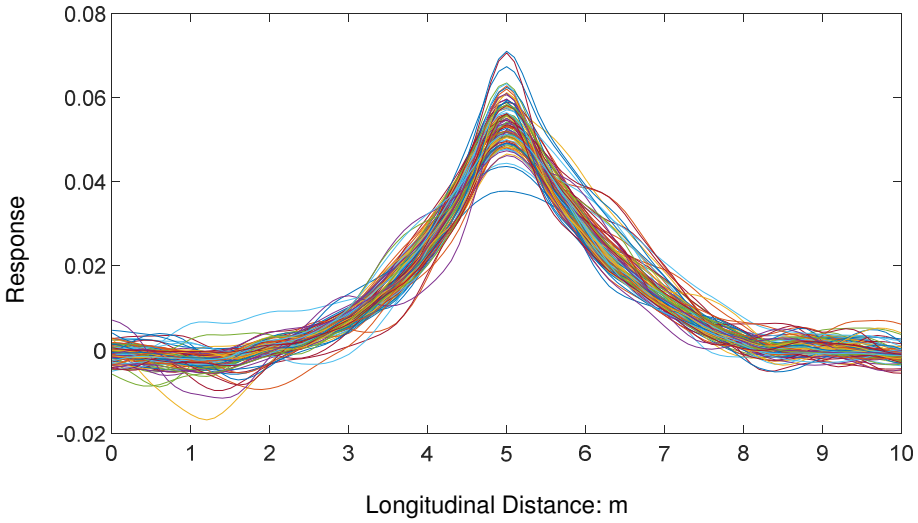

Figure 9: Measured ILs

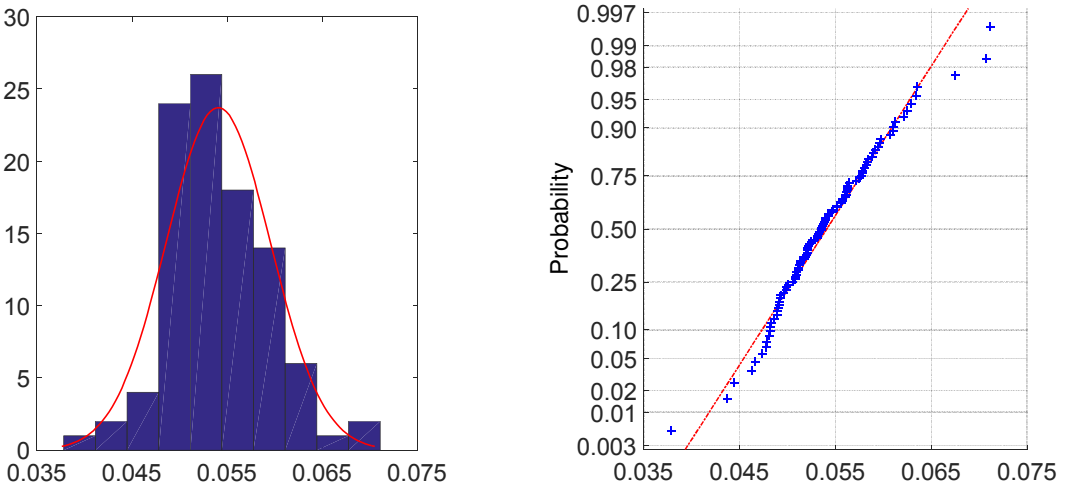

(a) Histogram **(b) Normal probability paper plot**

Figure 10: Normal distribution fit to the peak value of the influence line

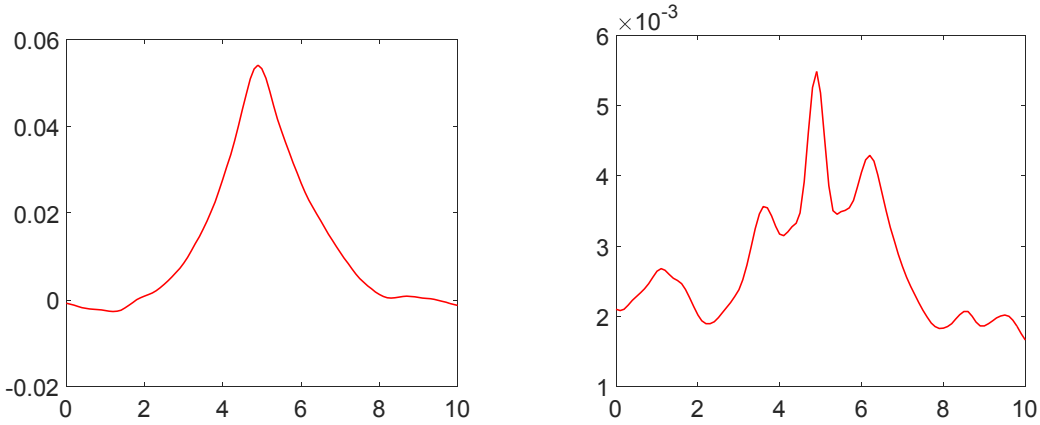

(a) Mean **(b) Standard deviation**

Figure 11: The means and standard deviations of measured influence line ordinates

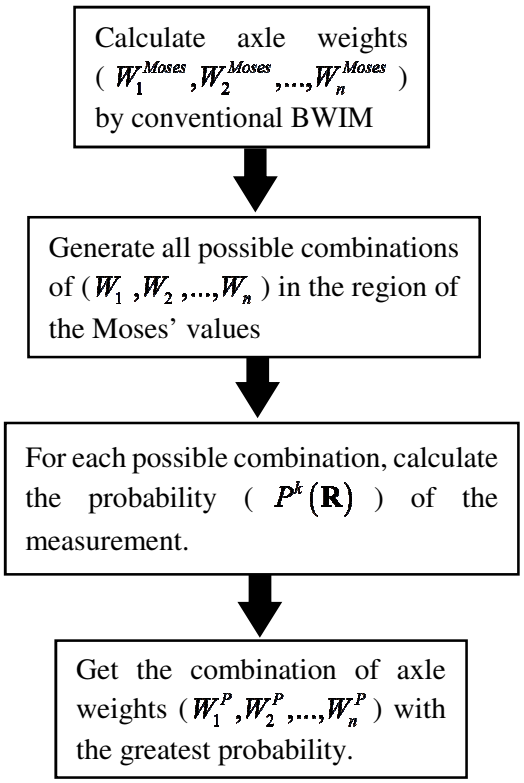

Figure 12: Flow chart of axle weight calculation using pBWIM

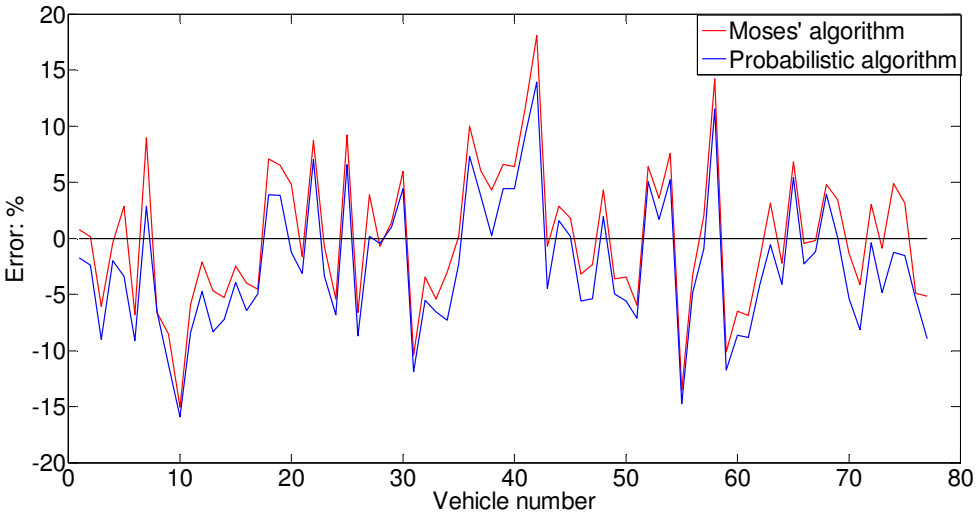

Figure 13: GVW error for each vehicle with two algorithms